

# Deeper Than You Think: Partisanship-Dependent Brain Responses in Early Sensory and Motor Brain Regions

Noa Katabi,<sup>1</sup> Hadas Simon,<sup>2</sup> Sharon Yakim,<sup>2</sup> Inbal Ravreby,<sup>2,3</sup> Tal Ohad,<sup>1</sup> and Yaara Yeshurun<sup>1,2</sup>

<sup>1</sup>Sagol School of Neuroscience, <sup>2</sup>School of Psychological Sciences, Tel-Aviv University, Tel Aviv, 6997801, Israel, and <sup>3</sup>Department of Neurobiology, Weizmann Institute of Science, Rehovot, 7610001, Israel

Recent political polarization has illustrated how individuals with opposing political views often experience ongoing events in markedly different ways. In this study, we explored the neural mechanisms underpinning this phenomenon. We conducted fMRI scanning of 34 right- and left-wing participants (45% females) watching political videos (e.g., campaign ads and political speeches) just before the elections in Israel. As expected, we observed significant differences between left- and right-wing participants in their interpretation of the videos' content. Furthermore, neuroimaging results revealed partisanship-dependent differences in activation and synchronization in higher-order regions. Surprisingly, such differences were also revealed in early sensory, motor, and somatosensory regions. We found that the political content synchronized the responses of primary visual and auditory cortices in a partisanship-dependent manner. Moreover, right-wing (and not left-wing) individuals' sensorimotor cortex was involved in processing right-wing (and not left-wing) political content. These differences were pronounced to the extent that we could predict political orientation from the early brain-response alone. Importantly, no such differences were found with respect to neutral content. Therefore, these results uncover more fundamental neural mechanisms underlying processes of political polarization.

**Key words:** brain; fMRI; IS-RSA; ISC; naturalistic stimuli; partisanship

## Significance Statement

The political sphere has become highly polarized in recent years. Would it be possible to identify the neural mechanisms underpinning such processes? In our study, left- and right-wing participants were scanned in fMRI while watching political video clips just before the elections in Israel. We found that political content was potent in synchronizing the brain responses of individuals holding similar views. This was far more pronounced in individuals holding right-wing views. Moreover, partisan-dependent differences in neural responses were identified already in early sensory, somatosensory, and motor regions, and only for political content. These results suggest that individuals' political views shape their neural responses at a very basic level.

## Introduction

Today, perhaps more than ever, creating a shared understanding of the world we live in seems like an urgent yet elusive endeavor. Humans understand each other well enough to create social and technological feats of immense complexity, but not enough to agree on whether the media coverage of an election was biased, or in which way. In this study, we study the neural mechanisms

that give rise to partisanship-dependent understanding of real-life political events.

Political partisanship influences one's choices, perception, and understanding of information (Cohen, 2003; Jost and Amodio, 2003; Carney et al., 2008; Frenda et al., 2013; Bolsen et al., 2014; Kraft et al., 2015; Jost et al., 2018; van Bavel and Pereira, 2018). These behavioral partisan-based differences were further borne out in neuroimaging studies. Previous studies found political-based differences in brain responses, as well as in the volume of specific regions (Jost and Amodio, 2003). For example, liberalism was associated with increased anterior cingulate (ACC) volume, and conservatism with increased amygdala volume (Kanai et al., 2011). These extend previous neurocognitive findings about the high degree of conflict-monitoring among liberals, which is associated with increased ACC activation (Amodio et al., 2007), and conservatives' sensitivity to threatening situations and facial expressions, which was reflected by emotional processing in areas,

Received May 10, 2022; revised Dec. 14, 2022; accepted Dec. 22, 2022.

Author contributions: N.K., S.Y., and T.O. analyzed data; N.K. and Y.Y. wrote the first draft of the paper; N.K., I.R., and Y.Y. edited the paper; N.K. and Y.Y. wrote the paper; H.S., S.Y., I.R., and Y.Y. designed research; H.S., S.Y., I.R., and Y.Y. performed research.

This work was supported by the Israel Science Foundation Grant 2434/19 to Y.Y. We thank Yohay Zvi, Dvir Caspi, and Muhammad Badarnee for assistance in scanning and data analysis.

The authors declare no competing financial interests.

Correspondence should be addressed to Yaara Yeshurun at yaaray@tauex.tau.ac.il.

<https://doi.org/10.1523/JNEUROSCI.0895-22.2022>

Copyright © 2023 the authors

such as the amygdala (Jost et al., 2003; Vigil, 2010). Differences such as these enabled prediction of political orientation based on the neural response, whether to disgusting images (Ahn et al., 2014), or in a risk-taking task (Schreiber et al., 2013).

Partisanship-dependent differences in brain response were also demonstrated in the context of naturalistic stimuli, such as stories and movies. For example, polarized political videos about immigration policy resulted in “neural polarization” (divergence in brain activity between liberals and conservatives) in the dorsal medial prefrontal cortex (dmPFC) (Leong et al., 2020). Similarly, a functional near-infrared spectroscopy (fNIRS) study in which participants watched videos on abortion could classify participants’ political views based on response patterns in the dmPFC (Dieffenbach et al., 2021). Moreover, a recent study examined the neural synchronization between individuals watching political and nonpolitical video clips (van Baar et al., 2021). In this study, participants who shared a political ideology had increased neural synchrony in regions, including the default mode network (DMN) for high-intensity political clips but not for low-intensity or nonpolitical clips. These findings are in line with previous research on interpretation-dependent responses of the DMN while processing nonpolitical movies and stories (Yeshurun et al., 2017; Finn et al., 2018; Nguyen et al., 2019). These previous studies did not directly compare partisan-dependent differences in neural synchronization across groups (i.e., left-wing vs right-wing).

In the present study, we tested how political partisanship shapes the brain response to polarizing political stimuli. By using fMRI, we were able to examine neural activation and synchronization of right- and left-wing participants while they watched various political video clips. Based on previous studies (Yeshurun et al., 2017; Nguyen et al., 2019; Leong et al., 2020; van Baar et al., 2021), we hypothesized that there would be partisan-dependent differences in the DMN while processing political content. Because of our focus on individuals with high levels of political engagement, and the timing of the experiment, just before the 2019 elections in Israel when political partisanship was intensified and almost omnipresent, we hypothesized that such differences may emerge already at early brain processing.

## Materials and Methods

### Participants

Forty-one right-handed participants took part in this fMRI study (24 males and 17 females, mean age =  $26.5 \pm 5.75$ ). Before taking part in the study, participants completed a questionnaire that included a question about their political involvement (“How much are you politically involved?”) which they answered using a visual analog scale (VAS) ranging from “not at all” (0) to “very much” (100) and a question regarding their political orientation (“How would you define your political orientation?”) which they answered using a VAS ranging from “Left” (0) to “Right” (100). We recruited individuals who were highly politically involved (mean = 75.62, SD = 23.87), and were markedly left-wing (mean = 15.29, SD = 11.82) or right-wing (mean = 86.59, SD = 12.9) (see Fig. 1a). Seven participants were discarded from the analysis: 4 because of our inability to characterize their political views based on their post-scan questionnaire, 2 because of incidental clinical findings, and 1 because of excessive head motion (>2 mm). The remaining 34 participants were divided into two equal groups based on their political views: Right-wing group (11 males and 6 females, mean age =  $27 \pm 6.4$ ) and Left-wing group (8 males and 9 females, mean age =  $24.88 \pm 3.8$ ). This sample size of 17 participants in each group has been shown in previous studies to be sufficient to test for similarities and differences in neural responses to naturalistic stimuli (Ames et al., 2015; Yeshurun et al., 2017), and for power analyses of intersubject correlation (Pajula and Tohka, 2016). In two (of the five) stimuli

we analyzed, we excluded a further 2 participants because of a lack of data following technical problems. The experimental procedures were approved by Tel Aviv University’s Ethics Committee and the Institutional Review Board at the Sheba Tel-Hashomer Medical Center. All participants provided written informed consent and received payment for their time.

### Stimuli and experimental design

The experiment took place 3 weeks before the April 2019 national elections in Israel. Participants watched 8 video clips inside the MRI scanner (mean length = 197 s, SD = 64.92 s): one neutral clip (a short documentary about someone who moved an old bus into his house); four campaign ads (two from a right-wing, one from a center, and one from a left-wing party); two political speeches (one by Benjamin Netanyahu, a right-wing politician; and one by Shelly Yachimovich, a left-wing politician); and a pre-election political survey clip. Each clip was preceded and followed by a gray screen: 8 s before, and 10 s after (which were discarded from the analysis).

After each clip, participants were asked to answer three questions about it: (1) “How much did you agree with the main message of this clip?” (2) “How much did this clip interest you?” and (3) “How emotionally engaged were you?” (see Fig. 1a). They answered these questions by indicating their ratings (using a magnet-compatible mouse) on a VAS that ranged from “Not at all” (0) to “Very” (100). The order of the clips was randomized into four versions, which all began with the neutral clip and ended with the political survey one. The participants’ eye gaze was monitored online and recorded at 500 Hz using SR-Research’s EyeLink 1000 Plus Eye-Tracker. However, because of technical issues, eye-tracking data were not collected in over half of the participants (18 of 34 participants), so we did not analyze that data. Immediately after the scan, participants completed a behavioral assessment session, that was held in a separate, adjacent room. In this session, there were 29 comprehension questions and 61 interpretation questions about the clips presented in the scanner, as well as general feelings and views about the politicians shown in the clips.

In this study, we analyzed the brain responses to five of the eight video clips (see Fig. 1a): neutral clip (Neutral, 151 s long); two right-wing clips: a right-wing campaign ad (RWC, 198 s long) and a right-wing politician’s speech (RWS, 235 s long); and two left-wing clips: a left-wing campaign ad (LWC, 206 s long) and a left-wing politician’s speech (LWS, 312 s long).

### MRI acquisition

Participants were scanned using a 3T Siemens Prisma scanner with a 64-channel head coil. T1-weighted structural images were acquired using a MPRAGE pulse sequence as follows: TR = 2530 ms, TE = 2.88 ms, TI = 1100 ms, flip angle =  $7^\circ$  and 250 Hz/px, isotropic voxel size of  $1 \text{ mm}^3$ . For functional scans, images were acquired by means of a T2\*-weighted multiband EPI protocol. TR = 1000 ms, TE = 34 ms, flip angle =  $60^\circ$ , multiband acceleration factor of six without parallel imaging. Isotropic resolution was  $2 \text{ mm}^3$  (no gaps) with full brain coverage; slice-acquisition order was interleaved.

### Imaging analysis

**Preprocessing.** Raw DICOM format imaging data were converted to Nifti with the dcm2nii tool. The Nifti files were organized according to the BIDS format version 1.0.1 (Gorgolewski et al., 2016). fMRI data preprocessing was conducted using the FMRIB’s Software Library’s (FSL version 6.0.2) fMRI Expert Analysis Tool (FEAT version 6.00) (Smith et al., 2004). All data were subjected to the following preprocessing procedures: brain extraction for skull-stripping anatomy image; slice-time correction; high-pass filtering (two cycles per stimulus’s length); motion correction to the middle time point of each run; and smoothing with a 4 mm FWHM kernel. All images were registered to the high-resolution anatomic data using boundary-based reconstruction and normalized to the MNI template, using nonlinear registration. BOLD response was normalized (z-scored) within subjects for every voxel for each video clip. HRF was calculated for each participant according to the peak start time of the BOLD response in early auditory areas (A1+), using the pre-

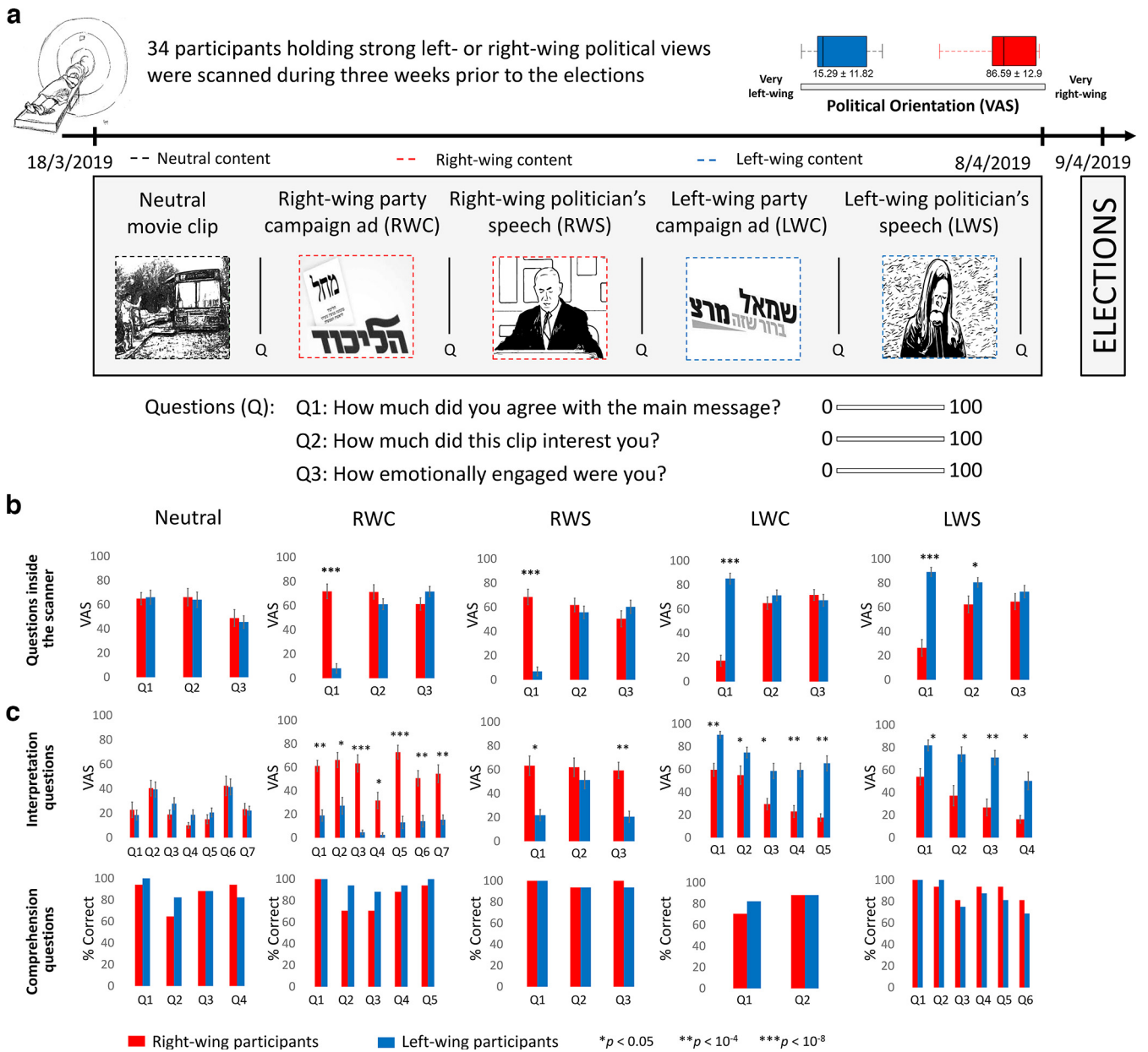


**Figure 1.** Stimuli and behavioral results. Left- and right-wing participants watched (**a**) five video clips inside the fMRI scanner and following each clip answered three questions: “How much did you agree with the main message of this clip?” “How much did this clip interest you?” “How emotionally engaged were you?” **b**, Participants’ ratings for these three questions demonstrated large differences between the two groups in terms of how much they agreed with the main message of the political clips, and relatively similar emotional engagement and interest with the clips. **c**, Graphs in top row represent post-scan questionnaires’ interpretation questions. Significant differences were found in each interpretation question for the political clips (except from one question in RWS). Graphs in bottom row represent post-scan questionnaires’ comprehension questions, in which there was no significant difference between the groups. Error bars indicate SE.

election political survey video clip (which was not part of the stimuli analyzed in this study). The shift was then calculated as the duration from the stimulus onset to the first peak of the hemodynamic response in A1+ (mean shift = 3.18 s, SD = 0.72). We further analyzed the data only in voxels that had a reliable BOLD signal (<3000 AU) in at least 90% of the participants in each group (right- and left-wing). This procedure resulted in 217,930 voxels for the neutral video clip, 214,919 voxels for the RWC video clip, 217,149 voxels for the LWC video clip, 217,232 voxels for the RWS, and 217,305 voxels for the LWS. Next, we divided the brain into 268 nodes, including cortical and subcortical regions, using a parcellation map based on resting-state connectivity (Shen et al., 2013). Within each node, we averaged the BOLD responses of all reliable voxels of each participant, for each video clip.

**Intersubject correlation.** We used intersubject correlation (ISC) (Hasson et al., 2004) to define nodes that were involved in processing the video clips (Neutral, RWC, RWS, LWC, and LWS). ISC measures

the degree to which neural responses to naturalistic stimuli are shared between participants processing the same stimuli. For each node, we correlated each participant’s time course with the average time course response across all other participants in the same group using Pearson correlation. We then averaged these 17 correlations coefficients values (or 16 values for RWS and LWS) to get an estimation of the in-group similarity in neural response for each of the 268 nodes. To determine whether a specific ISC value was significantly greater than chance, we calculated a null distribution generated by a bootstrapping procedure. For each of the video clips, for each empirical time course at each node, 1000 bootstrap-time series were generated using a phase-randomization procedure. Phase randomization was performed by Fast Fourier Transform (FFT) of the signal, randomizing the phase of each Fourier component, and then inverting the Fourier transformation back to the time domain. This procedure leaves the power spectrum of the signal unchanged but removes temporal alignments of

the signals. Using these bootstrap-time courses, a null distribution of the average correlations was calculated for each node.

To correct for multiple comparisons, we selected the highest ISC value from the null distribution in each node (Regev et al., 2013). The chosen threshold for every group, in each stimulus, was defined as the top 5% of the maximum values in the 268 nodes (Neutral threshold ISC: right-wing group  $> 0.15$ , left-wing group  $> 0.15$ ; RWC threshold ISC: right-wing group  $> 0.13$ , left-wing group  $> 0.13$ ; RWS threshold: right-wing group  $> 0.12$ , left-wing group  $> 0.12$ ; LWC threshold ISC: right-wing group  $> 0.14$ , left-wing group  $> 0.14$ ; LWS threshold: right-wing group  $> 0.11$ , left-wing group  $> 0.12$ ). These thresholds were used to test for regions that were involved in processing the video clips in each partisan group.

#### Testing between-groups differences in processing the stimuli

To test for differences in neural processing of the video clips, we first identified (in each clip) nodes in which only one of the groups had passed the ISC threshold while the other group did not (i.e., nodes that were involved in processing the clip only in one group and not in the other). Next, to verify that these nodes indeed reflected significant differences between the groups (i.e., it is not the case that the ISC value was just above the threshold in one group and just below the threshold in the other), we calculated the ISC value of each participant in each group by correlating between participant's response to the mean response of the group. We then applied Fisher transformation to these correlation coefficients and computed an independent sample two-tailed  $t$  test between the groups (i.e., comparing 17 values of right-wing participants with 17 values of left-wing participants). This resulted in a  $p$  value for each node. To correct for multiple comparisons, false discovery rate (FDR) (Benjamini and Hochberg, 1995) correction was applied with  $q$  criterion  $< 0.05$ .

#### Support-vector machine (SVM) classification

We trained an SVM classifier (Cortes and Vapnik, 1995) to test whether participants' partisanship can be classified according to the level of neural synchronization they share with their group while watching political content. We did so for each of the four political videos ( $N = 17$  in each group in RWC and LWC;  $N = 16$  in each group in RWS and LWS), in each of the 268 nodes. This classifier was a leave-two-out algorithm that received a training set and a testing set. We used one-dimensional space data, the correlation between each participant's brain response to the video and the averaged brain response of the rest of the group, to classify the participants' political views. The training set contained  $N-1$  correlation coefficients of each group, and the testing set contained the remaining two correlation coefficients (one from each political group). The support vector classifier used the training dataset to find a single point to serve as the hyperplane that classified the data into classes, and labeled the testing set as right- or left-wing accordingly. This algorithm was executed  $N^2$  times (each time, two different participants were left out). At each time, the classifier could be correct (1) or incorrect (0). The classifier accuracy in a specific node was the average of the  $N^2$  trials (e.g., a number between 0 and 1).

To test whether the classifier accuracy value was significantly larger than would be expected by chance, we simulated a null distribution using a permutation method. The data (16 or 17 within-group correlations for each group) from a specific node were extracted, and the labels of the groups were shuffled randomly to create two new pseudo groups. We then classified each participant's partisanship using the same classification procedure that was applied to the empirical data. This procedure of label shuffling and classifying was repeated 1000 times. Thus, we obtained a null distribution of 1000 classifier accuracies under the null hypothesis. This distribution reflects the probability of the classifier achieving a classification rate by chance. The  $p$  values of the empirical classifier accuracies were computed using the following formula: (number of null values larger than the real value + 1)/1000. We corrected for multiple comparisons by controlling FDR correction (Benjamini and Hochberg, 1995) with a  $q$  criterion of 0.05.

#### Intersubject representational similarity analysis (IS-RSA)

We used IS-RSA (Finn et al., 2020) to test whether stronger political views were associated with more similar brain responses to the political

video clips. Similarity in strength of political views was calculated using the AnnaK model (Finn et al., 2020). For each video clip, and for each pair of participants, we calculated their averaged agreement value with the main message of the video clip during the scan, which was rated using a VAS, ranging from 0 = Highly disagree to 100 = Highly agree. This resulted in a  $34 \times 34$  similarity matrix for the RWC and LWC, and a  $32 \times 32$  similarity matrix for the RWS and LWS. For the brain activity similarity matrix, we used the ISC method and computed a pairwise Pearson correlation between each pair of participants' time courses, for each node (for RWC and LWC:  $34 \times 34$  brain activity similarity matrices; for RWS and LWS:  $32 \times 32$  brain activity similarity matrices). The IS-RSA was then computed as the Spearman correlation between the behavioral matrix and the brain activity similarity matrix.

To determine whether a specific IS-RSA value was significantly greater than chance, we calculated a null distribution generated by a bootstrapping procedure. For each video clip, in each node, we generated a pseudo neural similarity matrix by choosing the time course of one participant, scrambled this participant's time course using a phase-randomization procedure, and then calculated pairwise correlation between this participant's scrambled time course with each of the other (33) participants' intact time courses. This resulted in a vector of  $1 \times 34$  pairwise correlation values per participant. We repeated this procedure for each of the 34 participants, resulting in a  $34 \times 34$  neural similarity matrix. This procedure kept the dependence structure of the neural similarity matrix, as each participant contributed to multiple cells in the matrix (as was the case in the real data similarity matrix). We then computed Spearman's correlation between the "pseudo" similarity brain matrix and the behavioral matrix. We repeated the phase randomization procedure 1000 times, to generate a null distribution of pseudo IS-RSA values for each node. The  $p$  values of the empirical Spearman's  $r$  values were computed using the following formula: (number of null values larger than the real value + 1)/1000. To correct for multiple comparisons, FDR correction (Benjamini and Hochberg, 1995) was applied, with a  $q$  criterion  $< 0.05$ .

#### Intersubject functional connectivity (ISFC)

To test whether political views were associated with stronger connectivity between brain regions, we used ISFC (Simony et al., 2016). To do so, we first defined ROIs as 10 nodes that were revealed by the ISC and IS-RSA analysis to have political-dependent responses and were in particular interest for the findings of this study. These nodes included parcels within the: primary visual cortex, bilateral auditory cortex, somatosensory cortex, motor cortex, pre-supplementary motor area (pre-SMA) and SMA, posterior cingulate cortex (PCC), right temporal parietal junction (TPJ), and dmPFC. For each of the 10 ROIs, for each participant, we extracted the time course and correlated it with the averaged time course of the remaining participants, in each of the 10 ROIs. These correlation values underwent a Fisher's  $r$ -to- $z$  transformation, were averaged across participants and then inverse transformed to produce averaged correlation values. This resulted in a  $10 \times 10$  ISFC matrix, of the functional connectivity between these 10 regions, and it was asymmetric because of the directional nature of this procedure. However, functional connectivity is considered to be unidirectional. Therefore, the symmetry was imposed by averaging the upper and the lower triangles (Simony et al., 2016).

Moreover, to test whether the functional connectivity between these ROIs was stronger in one group than the other, we completed a  $t$  test for independent samples. To do so, we used the previously defined ROIs' time courses of every participant. Each such time course of every participant was correlated with the averaged (across participants) time courses of all other ROIs. Next, these correlations underwent a Fisher's  $r$ -to- $z$  transformation, resulting in each edge having as many transformed correlations as there were participants. For every edge, we computed an independent sample two-tailed  $t$  test between the groups (i.e., comparing 17 values of right-wing participants with 17 values of left-wing participants). This resulted in a  $p$  value for each edge. To correct for multiple comparisons, FDR correction (Benjamini and Hochberg, 1995) was applied to all  $p$  values of all video clips with  $q$  criterion  $< 0.05$ .

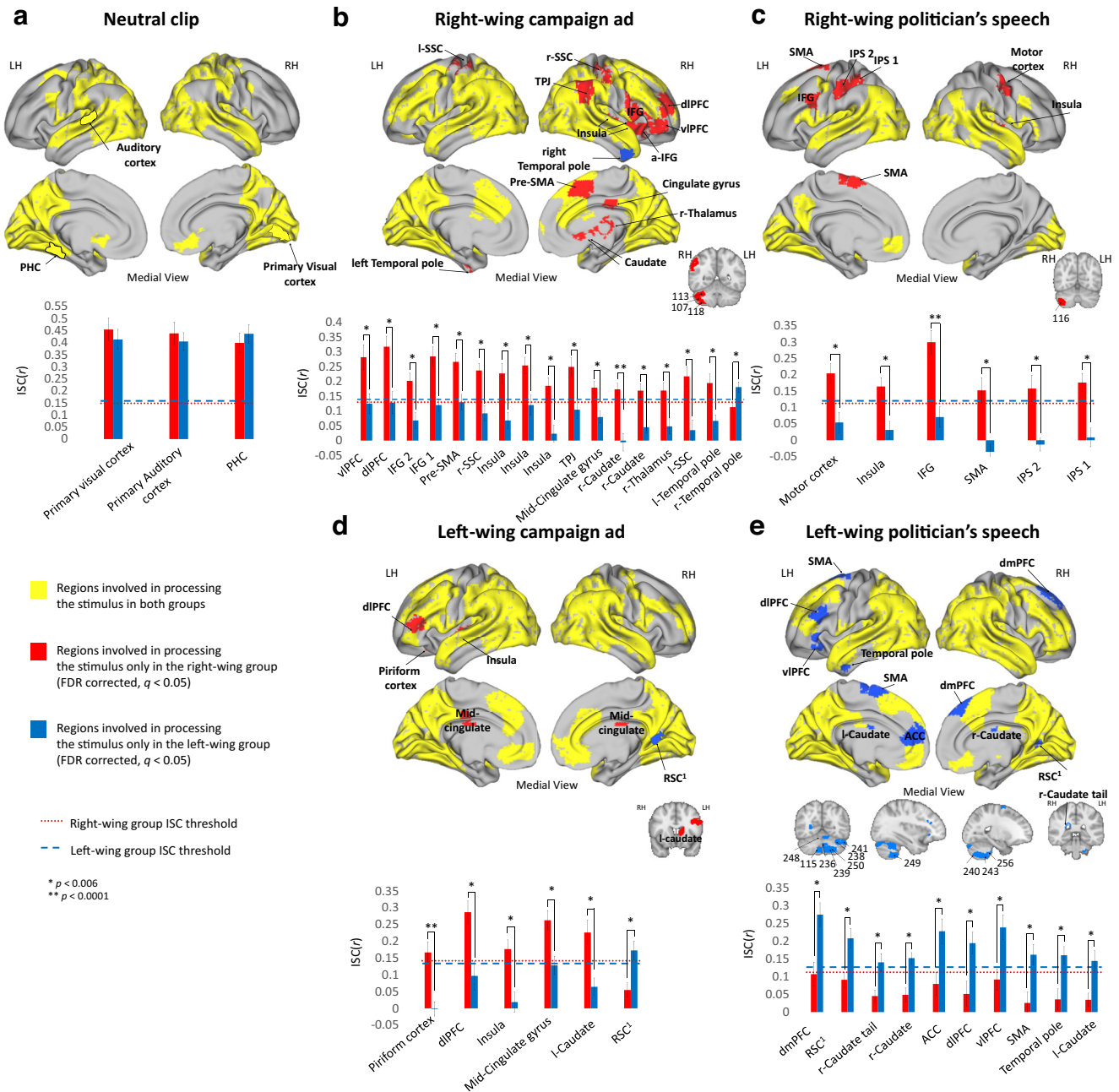


**Figure 2.** Similarities and differences in regions involved in processing the video clips. ISC analysis for the (a) Neutral video clip, (b) RWC, (c) RWS, (d) LWC, and (e) LWS. Top panels represent brain maps demonstrating regions involved in processing the stimuli in both groups (overlap between both groups ISC, yellow), only in the right-wing group (red), or only in the left-wing group (blue). Bottom panels represent ISC Pearson  $r$  values of both groups in each of the “red” and “blue” brain regions (mean  $\pm$  SE). Dashed lines indicate the group’s ISC threshold. All results are FDR-corrected ( $q < 0.05$ ). IPS, Intraparietal sulcus; IFG, inferior frontal gyrus; SSC, somatosensory cortex; vIPFC, ventrolateral prefrontal cortex; PHC, para-hippocampus cortex; RSC, adjacent to the retrosplenial cortex; LH, left hemisphere; RH, right hemisphere.

**Results**

**Partisanship-dependent differences in agreeing with the main messages of the video clip**

Participants’ ratings after watching each video clip in the scanner revealed that, while the right- and left-wing groups did not differ in the degree of their agreement with the main message of the neutral movie (left-wing group mean = 66.1, SD = 23.8, right-wing group mean = 64.97, SD = 20.86,  $t_{(32)} = 0.14$ ,  $p = 0.88$ ), there was a large and significant difference in their degree of agreement with the main message of the political video clips. Right-wing participants agreed much more with the main message of the right-wing content (RWC: left-wing group mean = 8.14, SD = 15.91,

right-wing group mean = 71.83, SD = 24.77,  $t_{(32)} = -8.92$ ,  $p < 10^{-9}$ ; RWS: left-wing group mean = 6.88, SD = 14.82, right-wing group mean = 68.49, SD = 26.29,  $t_{(32)} = -8.41$ ,  $p < 10^{-8}$ ), and left-wing participants agreed much more with the main message of the left-wing content (LWC: left-wing group mean = 85.17, SD = 18.07, right-wing group mean = 17.32, SD = 18.60,  $t_{(32)} = 10.78$ ,  $p < 10^{-11}$ ); LWS: left-wing group mean = 89.19, SD = 15.21, right-wing group mean = 26.40, SD = 28.28,  $t_{(32)} = 8.06$ ,  $p < 10^{-8}$ ) (Fig. 1b). Moreover, although there was a large difference in how much the partisan groups agreed with the message of the clips, there were no significant differences in the degree to which they were interested or emotionally engaged by them, except

Table 1. ISC results<sup>a</sup>

|                                       | Brain region                                      | Parcel number             | Right-wing group r value | Left-wing group r value | p value     |
|---------------------------------------|---------------------------------------------------|---------------------------|--------------------------|-------------------------|-------------|
| RWC                                   | Ventrolateral PFC <sup>b</sup>                    | 8                         | 0.281663618              | 0.124647609             | 0.005740883 |
|                                       | dIPFC <sup>b</sup>                                | 9                         | 0.317106272              | 0.127869051             | 0.000680215 |
|                                       | Inferior frontal gyrus 2 <sup>b</sup>             | 16                        | 0.201838607              | 0.067854314             | 0.000997031 |
|                                       | Inferior frontal gyrus 1 <sup>b</sup>             | 21                        | 0.284261697              | 0.11984986              | 0.000177213 |
|                                       | Pre-SMA <sup>b</sup>                              | 28                        | 0.265853675              | 0.129722755             | 0.001480891 |
|                                       | Right somatosensory cortex <sup>b</sup>           | 33                        | 0.236741798              | 0.091950018             | 0.000249812 |
|                                       | Insula <sup>b</sup>                               | 34                        | 0.226793931              | 0.06793036              | 0.001001179 |
|                                       | Insula <sup>b</sup>                               | 36                        | 0.253632625              | 0.120036147             | 0.004058332 |
|                                       | Insula <sup>b</sup>                               | 37                        | 0.185117948              | 0.023285424             | 0.000219385 |
|                                       | Temporal parietal junction <sup>b</sup>           | 47                        | 0.248938271              | 0.104259211             | 0.001838113 |
|                                       | Right temporal pole <sup>c</sup>                  | 57                        | 0.112859953              | 0.180711552             | 0.005745508 |
|                                       | Mid-cingulate gyrus <sup>b</sup>                  | 88                        | 0.178596062              | 0.079448883             | 0.001986054 |
|                                       | Right caudate nucleus <sup>b</sup>                | 121                       | 0.173126603              | −0.005745837            | 2.03E-05    |
|                                       | Right caudate nucleus <sup>b</sup>                | 123                       | 0.168722399              | 0.045106209             | 0.000323011 |
|                                       | Right thalamus <sup>b</sup>                       | 128                       | 0.168996137              | 0.048147906             | 0.002678115 |
|                                       | Left somatosensory cortex <sup>b</sup>            | 167                       | 0.216761205              | 0.035082372             | 0.000567027 |
|                                       | Left temporal pole <sup>b</sup>                   | 202                       | 0.194293245              | 0.066491606             | 0.001402024 |
|                                       | Cerebellum <sup>b</sup>                           | 107                       | 0.222779931              | 0.112676192             | 0.002041348 |
|                                       | Cerebellum <sup>b</sup>                           | 113                       | 0.286654288              | 0.10891178              | 1.92E-05    |
|                                       | Cerebellum <sup>b</sup>                           | 118                       | 0.200593547              | 0.098199341             | 0.001361587 |
|                                       | Premotor cortex <sup>b,d</sup>                    | 26                        | 0.292530619              | 0.181054906             | 0.005665347 |
|                                       | Somatosensory cortex 1 <sup>b,d</sup>             | 38                        | 0.360109424              | 0.202224634             | 0.001793549 |
| Somatosensory cortex 2 <sup>b,d</sup> | 45                                                | 0.381966359               | 0.238585623              | 4.26E-03                |             |
| Visual cortex <sup>b,d</sup>          | 82                                                | 0.426501239               | 0.290809337              | 0.00563985              |             |
| Parahippocampus gyrus <sup>b,d</sup>  | 198                                               | 0.492957399               | 0.391656067              | 0.004953297             |             |
| PCC <sup>b,d</sup>                    | 223                                               | 0.318108321               | 0.16844128               | 0.000839135             |             |
| LWC                                   | Adjacent to the retrosplenial cortex <sup>c</sup> | 87                        | 0.054760134              | 0.172599501             | 0.001834386 |
|                                       | Piriform cortex <sup>b</sup>                      | 135                       | 0.166635939              | −0.00164614             | 8.84E-05    |
|                                       | dIPFC <sup>b</sup>                                | 154                       | 0.286743133              | 0.09685222              | 1.35E-03    |
|                                       | Insula <sup>b</sup>                               | 170                       | 0.176572929              | 0.018787769             | 0.000530824 |
|                                       | Mid-cingulate cortex <sup>b</sup>                 | 224                       | 0.26267003               | 0.128300996             | 0.001866731 |
|                                       | Left caudate nucleus <sup>b</sup>                 | 258                       | 0.2261971                | 0.064225399             | 0.000982825 |
|                                       | Inferior frontal gyrus <sup>b,d</sup>             | 157                       | 0.376030084              | 0.203038404             | 1.33E-03    |
|                                       | Intraparietal sulcus 2 <sup>b,d</sup>             | 171                       | 0.352879518              | 0.156949755             | 2.74E-05    |
|                                       | Intraparietal sulcus 1 <sup>b,d</sup>             | 179                       | 0.438333498              | 0.241452459             | 5.03E-05    |
|                                       | RWS                                               | Motor cortex <sup>b</sup> | 27                       | 0.204692104             | 0.054304817 |
| Insula <sup>b</sup>                   |                                                   | 37                        | 0.164546285              | 0.031492065             | 0.001528941 |
| Inferior frontal gyrus <sup>b</sup>   |                                                   | 157                       | 0.300264174              | 0.071035343             | 3.81232E-05 |
| SMA cortex <sup>b</sup>               |                                                   | 162                       | 0.152740245              | −0.035782314            | 0.000230684 |
| Intraparietal sulcus 2 <sup>b</sup>   |                                                   | 171                       | 0.15823344               | −0.013339452            | 0.000640032 |
| Intraparietal sulcus 1 <sup>b</sup>   |                                                   | 179                       | 0.176638418              | 0.008657955             | 0.000235378 |
| LWS                                   | Right dmPFC <sup>c</sup>                          | 12                        | 0.106593352              | 0.27403593              | 0.001365341 |
|                                       | Adjacent to the retrosplenial cortex <sup>c</sup> | 87                        | 0.090844607              | 0.20754255              | 0.002105866 |
|                                       | Caudate nucleus tail <sup>c</sup>                 | 120                       | 0.045221768              | 0.139963159             | 0.003109876 |
|                                       | Right caudate nucleus <sup>c</sup>                | 122                       | 0.048601543              | 0.151721747             | 0.000310526 |
|                                       | ACC <sup>c</sup>                                  | 140                       | 0.079249108              | 0.227382029             | 0.004050548 |
|                                       | dIPFC <sup>c</sup>                                | 147                       | 0.05103565               | 0.193957963             | 0.005359024 |
|                                       | Ventrolateral PFC <sup>c</sup>                    | 151                       | 0.09153541               | 0.238192891             | 0.003260951 |
|                                       | SMA cortex <sup>c</sup>                           | 162                       | 0.025724141              | 0.16133073              | 0.002964581 |
|                                       | Temporal pole <sup>c</sup>                        | 194                       | 0.035776768              | 0.159820123             | 0.002889317 |
|                                       | Left caudate nucleus <sup>c</sup>                 | 260                       | 0.034553397              | 0.143986683             | 0.003256899 |
|                                       | Cerebellum <sup>c</sup>                           | 115                       | 0.089186464              | 0.175682416             | 0.000766296 |
|                                       | Cerebellum <sup>c</sup>                           | 236                       | 0.045861221              | 0.182617233             | 0.000914433 |
|                                       | Cerebellum <sup>c</sup>                           | 238                       | 0.062093042              | 0.241649461             | 0.000741513 |
|                                       | Cerebellum <sup>c</sup>                           | 239                       | 0.025576026              | 0.166012853             | 1.67E-05    |
|                                       | Cerebellum <sup>c</sup>                           | 240                       | 0.093581625              | 0.212110632             | 0.001662393 |
|                                       | Cerebellum <sup>c</sup>                           | 241                       | 0.106996004              | 0.273658258             | 0.005058712 |
|                                       | Cerebellum <sup>c</sup>                           | 243                       | 0.040104712              | 0.151942451             | 0.001598643 |
|                                       | Cerebellum <sup>c</sup>                           | 248                       | 0.10391465               | 0.241212581             | 0.003027496 |
|                                       | Cerebellum <sup>c</sup>                           | 249                       | 0.068352422              | 0.212039562             | 0.00177103  |
|                                       | Cerebellum <sup>c</sup>                           | 250                       | 0.020488189              | 0.217056111             | 8.61E-07    |
| Cerebellum <sup>c</sup>               | 256                                               | 0.053953807               | 0.143541337              | 0.003604706             |             |
| Medial frontal gyrus <sup>c</sup>     | 14                                                | 0.165683261               | 0.332680307              | 0.003518403             |             |
| Left dmPFC 1 <sup>c</sup>             | 145                                               | 0.119074572               | 0.287968377              | 0.001574639             |             |
| Left dmPFC 2 <sup>c</sup>             | 148                                               | 0.124787167               | 0.264546108              | 0.003726805             |             |

<sup>a</sup>All significant nodes are FDR-corrected ( $q < 0.05$ ).<sup>b</sup>Parcels that were significantly more correlated in the right-wing group.<sup>c</sup>Parcels that were significantly more correlated in the left-wing group.<sup>d</sup>Parcels that were involved in processing the stimulus in both groups but were significantly more correlated in one of them.

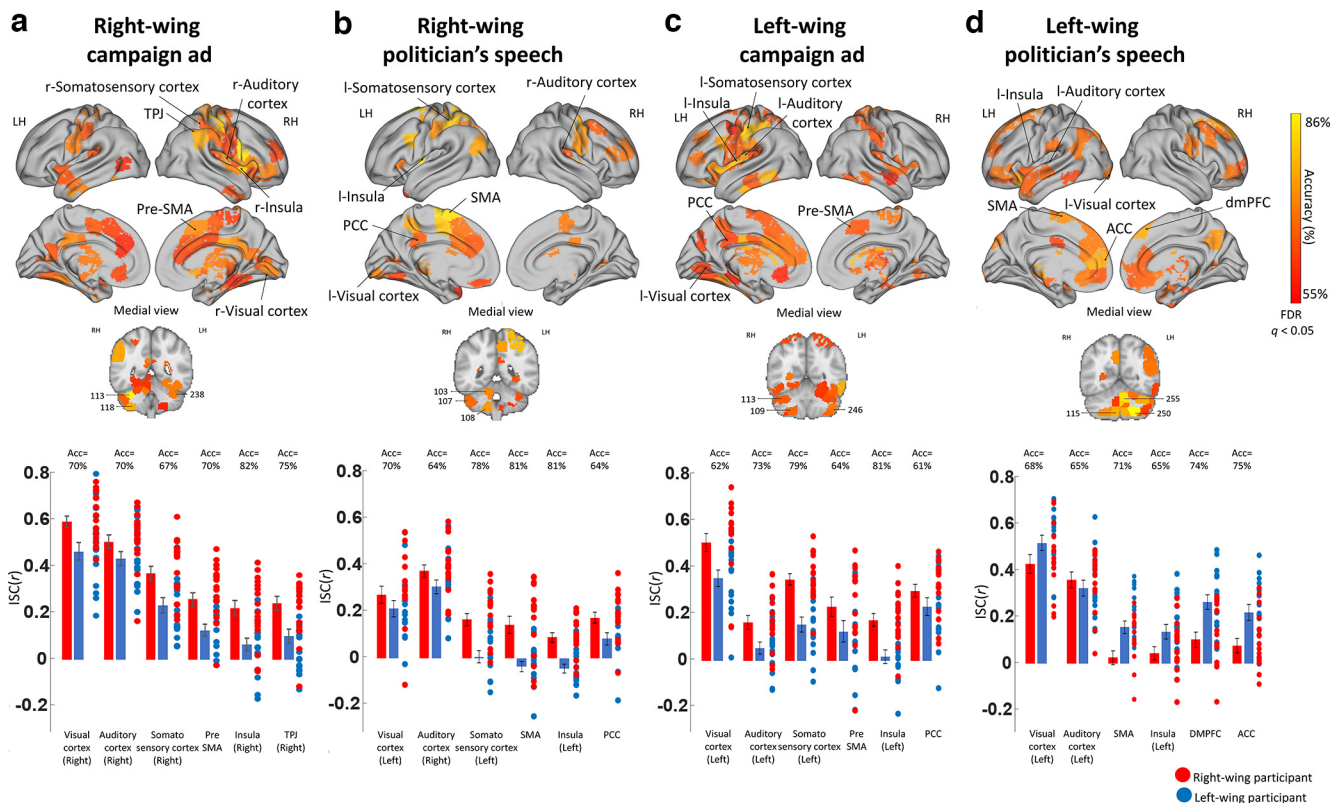


**Figure 3.** Classifying partisanship based on within-group synchronization. **a–d**, SVM classifier results for RWC, RWS, LWC, and LWS. Top panels, Brain maps demonstrating regions that significantly classified participant's partisanship according to their within-group synchronization (FDR-corrected,  $q < 0.05$ ). Bottom graphs, ISC Pearson  $r$  values of both groups (mean  $\pm$  SE), as well as the correlation coefficient of each participant's brain response with the averaged brain response of the rest of their group in six representative brain regions. LH, left hemisphere; RH, right hemisphere.

with regard to the LWS, which left-wing participants found to be more interesting (left-wing group mean = 80.54, SD = 16.49, right-wing group mean = 62.35, SD = 28.58,  $t_{(32)} = 2.27$ ,  $p < 0.05$ ) (Fig. 1*b*).

Post-scan questionnaires revealed that, while there were no significant differences between the groups in the interpretation of the neutral video clip, the two partisan groups significantly differ in how they interpreted the political video clips: RWC: (L-group mean = 19.64, SD = 18.48, R-group mean = 56.16, SD = 12.83;  $t_{(14)} = 2.14$ ,  $p = 0.0004$ ); RWS: (L-group mean = 31.25, SD = 17.43, R-group mean = 61.53, SD = 2.01;  $t_{(4)} = 2.77$ ,  $p = 0.04$ ); LWC: (L-group mean = 61.99, SD = 16.99, R-group mean = 38.98, SD = 16.15;  $t_{(12)} = 2.17$ ,  $p = 0.02$ ); and LWS: (L-group mean = 69.29, SD = 13.45, R-group mean = 33.59, SD = 16.06;  $t_{(6)} = 2.44$ ,  $p = 0.01$ ) (Fig. 1*c*). Moreover, these questionnaires revealed that the groups did not significantly differ on the comprehension questions (Fig. 1*c*).

### Partisanship-dependent differences in regions involved in processing the political content

To test for partisanship-dependent brain response similarities and differences in processing the stimuli, we first divided the brain into 268 nodes, using a parcellation map based on resting-state connectivity (Shen et al., 2013). We then tested the brain response to the neutral and political clips by using intersubject correlation (ISC) analysis (Hasson et al., 2004). Each of the five clips generated an extensive brain response among both groups, including primary visual and auditory cortex, the mentalizing network, and the lateral PFC (Fig. 2, yellow).

To test for regions that were involved in processing the stimuli only in one group and not in the other, we performed a two-step analysis (for details, see Materials and Methods). Notably,

we found political-group-dependent differences only with regard to the political clips, and not for the neutral clip (Fig. 2*a*). For the right-wing content, we found many regions (25 nodes) that were involved in processing the stimuli in the right-wing participants, but not in the left-wing participants (Fig. 2*b,c*, red).

These regions included right dorsolateral prefrontal cortex (dlPFC), TPJ, PCC, right caudate, as well as part of the somatosensory cortex, motor, and premotor areas. Only one node (right temporal pole in RWC; Fig. 2*b*, marked in blue) was involved in processing the clip in left-wing participants, but not right-wing participants.

For the left-wing clips, there was a substantial difference between the brain response to the campaign ad and to the politician's speech. For the left-wing campaign ad, we saw a similar pattern as for the right-wing clips, with five nodes, such as the insula and l-dlPFC, that were involved in processing the stimuli in the right-wing participants, but not in the left-wing participants (Fig. 2*d*, red; Table 1). Only one area, adjacent to the retrosplenial cortex was involved in processing the stimulus only in the left-wing group, and not in the right (Fig. 2*d*, blue).

For the left-wing politician's speech, there was an opposite pattern than that found for the other political content. Here, we found regions that were involved in processing the stimulus only within left-wing participants, but not within their right-wing counterparts (Fig. 2*e*, blue; Table 1). These included the dmPFC, ACC, ventrolateral PFC, and the cerebellum.

Together, these results suggest that, in addition to the expected DMN and high-order regions, partisanship-dependent differences were identified already in motor and somatosensory brain regions.

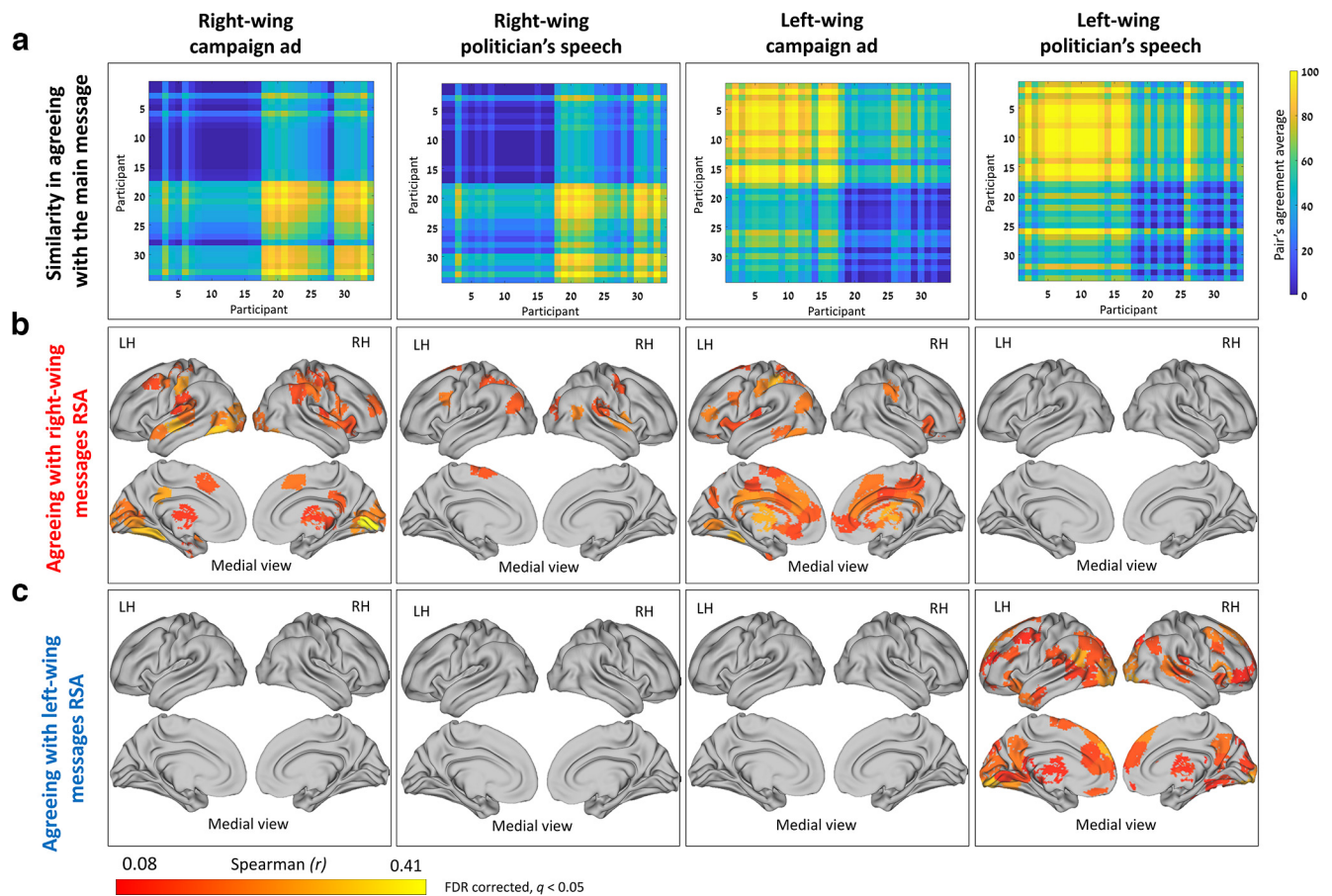


**Figure 4.** Higher neural synchronization associated with stronger political views. **a**, The matrices represent behavioral similarity based on “agreement with the main message.” **b**, The IS-RSA brain maps agreeing with a right-wing view revealed many regions that were more synchronized between participants holding strong right-wing views while processing the right-wing content and the left-wing campaign ad. **c**, The IS-RSA brain maps agreeing with a left-wing view revealed many regions that were more synchronized between participants holding strong left-wing views while processing the left-wing politician’s speech. Red to yellow brain areas represent areas with an  $r$  value  $\leq 0.407$  and FDR-corrected ( $q < 0.05$ ). LH, Left hemisphere; RH, right hemisphere.

### Partisanship-dependent neural synchronization

To further understand partisanship-dependent differences in the neural response, manifested in neural synchronization, we applied an SVM classifier and IS-RSA (Finn et al., 2020).

#### (1) Within-group neural synchronization predicts individual’s partisanship

We tested whether participant’s neural synchronization with their group would allow us to predict their political views (i.e., right- or left-wing). We did so using a very simple SVM classifier (for details, see Materials and Methods). We found significant classification accuracy in many brain regions: for the RWC, there were 88 such parcels, in which the classification accuracy ranged from 58% to 85% (Fig. 3a); for the RWS there were 43 such parcels, in which the classification accuracy ranged from 60% to 81% (Fig. 3b); for the LWC there were 82 such parcels, in which the classification accuracy ranged from 55% to 82% (Fig. 3c); for the LWS there were 80 such parcels, in which the classification accuracy ranged from 61% to 84% (Fig. 3d). Interestingly, in addition to regions within the DMN, the classifier achieved high accuracy rates (up to 85%) in visual, auditory, somatosensory, and motor cortices, as well as in the cerebellum (Fig. 3, bottom).

Consistent with the ISC results, for the right-wing clips and the left-wing campaign ad, in most regions with significant classification accuracy, there was a clear pattern of high correlation

within right-wing participants and low correlation within left-wing participants (Fig. 3a–c, bottom).

For the RWC, of the 88 parcels with significant classification accuracy, in 78 parcels there was higher synchronization within the right-wing group than within the left wing-group, and in 56 of these parcels this difference was significant. For the RWS, of the 43 parcels with significant classification accuracy, in 35 parcels there was higher synchronization within the right-wing group than within the left wing-group, and in 22 of these parcels this difference was significant.

An opposite pattern was identified for the left-wing politician’s speech, in which regions with significant classification accuracy had higher within-group synchronization for the left-wing group (Fig. 3d, bottom). For the LWS, of the 80 parcels with significant classification accuracy, in 70 parcels there was higher synchronization within the left-wing group than within the right wing-group, and in 46 of these parcels this difference was significant.

Together, these results suggest that an individual’s neural synchronization with other members of their partisanship group was enough to predict an individual’s political views.

(2) Stronger partisanship results in higher neural synchronization  
We applied IS-RSA (Finn et al., 2020) to test whether the stronger any two participants’ political views were (to the right or



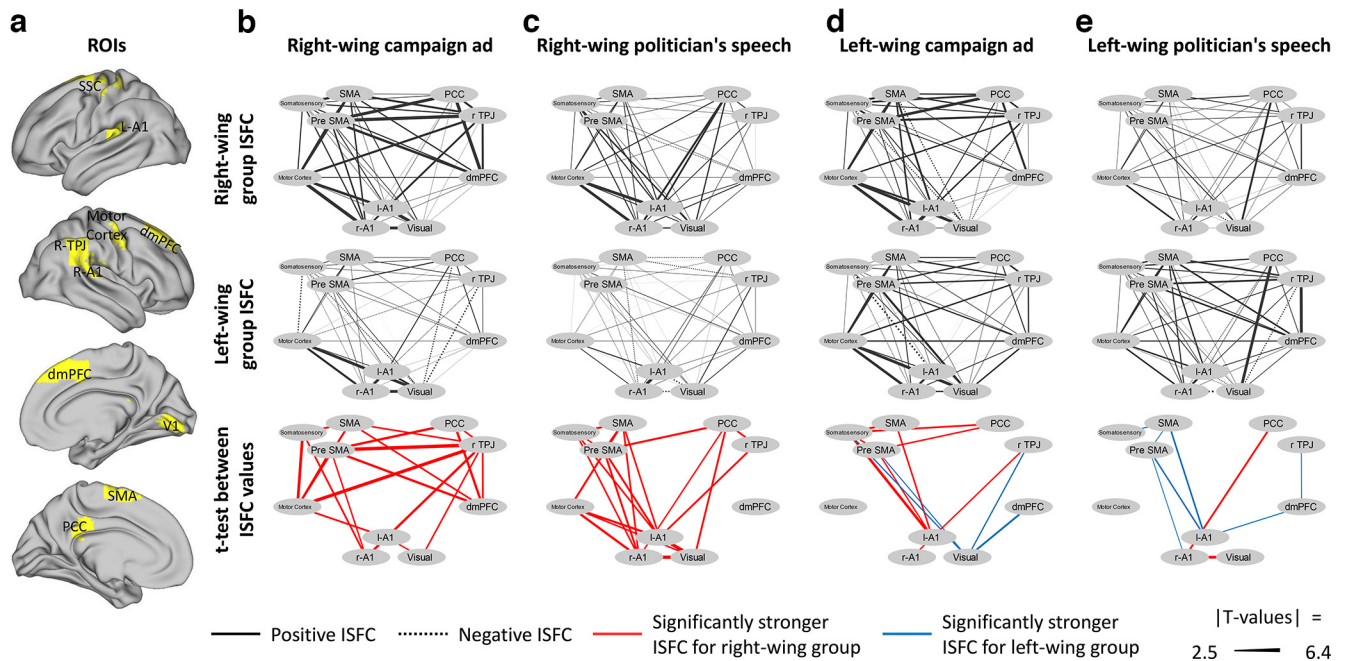


**Figure 5.** Functional connectivity between sensory, somatosensory, motor, and DMN regions. ISFC between (a) 10 ROIs (primary visual cortex, bilateral primary auditory cortex, somatosensory cortex, primary motor cortex, pre-SMA, SMA, dmPFC, right TPJ, and PCC) for the (b) right-wing campaign ad, (c) right-wing politician's speech, (d) left-wing campaign ad, and (e) left-wing politician's speech. Top, Functional connectivity within the right-wing group. Middle, Functional connectivity within the left-wing group. Bottom, The edges in which there was significantly higher connectivity within the right-wing group (compared with the left-wing group, red) or within the left-wing group (compared with the right-wing group, blue). All results are FDR-corrected ( $q < 0.05$ ).

left), the more similar were their brain responses. For each video clip, we generated political views similarity matrix by averaging each pair of participants' degree of agreement with the main message of the clip (Fig. 4a), and a brain similarity matrix, by calculating the pairwise correlation between every 2 participants. We then computed Spearman's rank correlation between the behavioral matrix and the brain-similarity matrix. Stronger right-wing views were associated with similar brain responses for most of the stimuli, particularly with regard to the political campaign ads (RWC and LWC) in many brain regions (Fig. 4b). These regions included areas within the DMN (e.g., TPJ and PCC), dmPFC and somatosensory cortices (similar regions to those identified in the ISC results), as well as primary visual area, primary auditory cortex, insula, fusiform, and subcortical regions (e.g., thalamus, caudate, and NAcc). We found that stronger left-wing views while processing the left-wing politician's speech, were associated with more synchronized brain activation in many brain regions, including the visual cortex, precuneus, dmPFC, ACC, orbitofrontal cortex, and thalamus (Fig. 4c).

Together, these results reveal that the content of the clips shaped the synchronization patterns of regions within the DMN (along partisan lines) and, more surprisingly, the synchronization of early sensory and somatosensory regions as well. Moreover, these synchronization patterns were more pronounced within participants sharing strong (right or left, depending on the content) political opinions.

### Partisanship-dependent differences in functional connectivity between sensory, somatosensory, motor, and DMN regions

The ISC and IS-RSA analysis revealed partisanship-dependent differences in the response of regions within the DMN as well as regions within the sensory, somatosensory, and motor regions. We used ISFC to test whether political views were associated

with stronger connectivity between 10 of these regions (Fig. 5a). This analysis revealed that, for the right-wing content, there was significantly higher functional connectivity among the right-wing group (compared with the left-wing group) in 20 edges for RWC and 20 edges for RWS, and 0 edges demonstrated the opposite pattern of higher connectivity in the left-wing group (Fig. 5b,c). As for the left-wing campaign ad, there was significantly higher functional connectivity among the right-wing group in 8 edges [left A1 and (1) somatosensory, (2) pre-SMA, (3) SMA, and (4) right TPJ; PCC and (5) somatosensory, (6) pre-SMA; and (7) SMA and somatosensory, and (8) right A1 and right TPJ] and significantly higher functional connectivity among the left-wing group in 4 edges [visual and (1) dmPFC, (2) rTPJ, (3) pre-SMA, and (4) somatosensory] (Fig. 5d). Finally, for the left-wing politician's speech, there was significantly higher functional connectivity among the right-wing group in 2 edges [right A1 with (1) visual and (2) PCC] and significantly higher functional connectivity among the left-wing group in 7 edges [left A1 with (1) pre-SMA, (2) SMA, and (3) dmPFC; SMA with (4) pre-SMA and (5) somatosensory; (6) right A1 and pre-SMA and (7) dmPFC and right TPJ; Fig. 5e]. The range of the significant functional connectivity T values was between 2.5 and 6.4.

Together, these results suggest that, while right-wing participants processed right-wing content, there was increased functional connectivity between many regions of the DMN, sensory, somatosensory, and motor cortices; and while left-wing participants processed left-wing content, there was increased functional connectivity between a few of these regions.

### Discussion

Our results demonstrated partisanship-dependent differences in brain activation and synchronization of individuals processing political content. These differences emerged already in early sensory,

somatosensory, and motor regions, and not only in the DMN, as was predicted in light of existing research.

The involvement of certain regions within the DMN, such as parts of the TPJ, PCC, and dmPFC, depended on the interplay between the political content and participants' political views. That is, they were involved only when right-wing participants watched the right-wing stimuli, or when left-wing participants watched the left-wing politician's speech. This is in line with prior studies that used nonpolitical narratives and found that the DMN was involved in comprehension and interpretation of naturalistic stimuli (Ames et al., 2015; Yeshurun et al., 2017; Finn et al., 2018; Nguyen et al., 2019). Moreover, recent studies suggested that dmPFC and TPJ responses differed between conservatives and liberals while they watched polarized political content (Dieffenbach et al., 2021; van Baar et al., 2021), and that this difference increased when emotional language was involved (Leong et al., 2020).

Our results revealed that the somatosensory, premotor, and motor regions were involved in processing the right-wing stimuli only in right-wing individuals (Fig. 2*b,c*). Moreover, there was increased connectivity between these regions and regions within the DMN, while right-wing individuals processed right-wing content (Fig. 5*b,c*). We interpret these findings through the lens of embodied cognition (Feldman and Narayanan, 2004), simulation theory (Jeannerod, 2001), and the bidirectional link between body movements and cognition (Neumann et al., 2003). It has been suggested that the sensorimotor experience is part of how an event is represented in the brain (Garbarini and Adenzato, 2004), as demonstrated by findings that people use sensorimotor representation to process action and nonaction words and sentences (Tettamanti et al., 2005; Marino et al., 2012) as well as facial expressions (Adolphs et al., 2000). Moreover, such simulative representation mechanisms allow a better understanding of other people's actions and intentions (Gallese, 2000; Blakemore and Decety, 2001). We suggest that our findings that right-wing individuals activated the somatosensory, premotor, and motor regions while processing right-wing content may imply that they used sensorimotor simulative representation to process this content. We further suggest that this representation may facilitate their identification with the right-wing content through a mechanism similar to that found in other studies among people who felt enhanced empathy for their in-group members who were experiencing pain (Xu et al., 2009; Hein et al., 2010). In other words, we argue that this potential sensorimotor representation allows the right-wing participants to better understand the intentions behind the actions of the main character in the right-wing movie clips, and identify with him.

Partisanship-dependent differences also emerged in the groups' neural synchronization. We found that we could classify a participant's political views based on the level of synchronization with their in-group members (Fig. 3) and that these differences in synchronization were more pronounced for participants holding stronger political views (Fig. 4). Moreover, most of the political stimuli were more potent in synchronizing the brain responses of individuals with right-wing views, while the left-wing politician's speech was more potent in synchronizing the brain responses of left-wing participants (Figs. 3 and 4). Notably, this pattern was striking in its dichotomy: agreeing with a right-wing message presented in most of the clips synchronized the participants' responses in many different brain regions, whereas in the same clips, agreeing with a left-wing message did not synchronize participant responses in any brain region (and vice versa for the left-wing politician's speech; Fig. 4). Specifically, the

results revealed that individuals' political outlook shaped synchronization in various brain regions, including the DMN, dlPFC, parahippocampus, somatosensory and motor regions, primary visual and auditory cortices, as well as in subcortical areas (Figs. 3 and 4). While these highly synchronized responses of the DMN and lateral PFC are in line with previous studies that found these regions to be involved in subjective interpretation (van Overwalle and Baetens, 2009; Bruneau et al., 2012; Skerry and Saxe, 2015; Yeshurun et al., 2017; Finn et al., 2018), and specifically in political contexts (Schmälzle et al., 2015; Leong et al., 2020; van Baar et al., 2021), we would like to focus on the unexpected increase in partisanship-dependent synchronization in primary sensory cortices.

We found partisanship-dependent synchronization in primary visual and auditory cortices (i.e., it was possible to predict one's political views based on their within-group synchronization in these regions). In other words, the political views of individuals shape their neural responses at a very basic level. Moreover, we found partisan-dependent differences in the functional connectivity between these primary sensory regions, and regions with the DMN (Fig. 5). These discrepancies in early-brain processing might result from top-down processes that lead to differences in attention; that is, participants' attention is likely to diverge according to their view of a given speaker (e.g., right-wing individuals will pay more attention to a right-wing speaker they endorse). These findings complement previous studies that found similar between-groups activation in primary sensory regions regardless of whether participants understood the narrative or not (Honey et al., 2012; Ames et al., 2015), or understood it in different ways (Schmälzle et al., 2015; Yeshurun et al., 2017; Leong et al., 2020; van Baar et al., 2021). We suggest that these effects, which have not been previously demonstrated, stem from participants' high levels of engagement and emotional reaction to the stimuli. These, in turn, may result from the timing of the experiment (3 weeks before the elections in Israel, when the political atmosphere was tense and fraught), and our recruitment of individuals that were politically involved to begin with. Our findings that political views shape the response of early-sensory regions may suggest that these regions are involved in processing high-level (and not merely low-level) aspects of external stimuli.

It is evident that the political sphere has become highly polarized in recent years (Leonard et al., 2021; Mason, 2015). Our finding of partisanship-dependent differences in activation and synchronization already in primary sensory and motor regions may contribute to our understanding of how such differences come about. In this study, we focused on political views, but our results could be relevant to any instance of partisanship. In this, we argue that these results can help us better understand the neural basis of group-based interpretive perspectives, and therefore potentially address multiple psychological and social challenges facing society.

## References

- Adolphs R, Damasio H, Tranel D, Cooper G, Damasio AR (2000) A role for somatosensory cortices in the visual recognition of emotion as revealed by three-dimensional lesion mapping. *J Neurosci* 20:2683–2690.
- Ahn WY, Kishida KT, Gu X, Lohrenz T, Harvey A, Alford JR, Montague PR (2014) Nonpolitical images evoke neural predictors of political ideology. *Current Biology* 24:2693–2699.
- Ames DL, Honey CJ, Chow MA, Todorov A, Hasson U (2015) Contextual alignment of cognitive and neural dynamics. *J Cogn Neurosci* 27:655–664.
- Amodio DM, Jost JT, Master SL, Yee CM (2007) Neurocognitive correlates of liberalism and conservatism. *Nature neuroscience* 10:1246–1247.

- Benjamini Y, Hochberg Y (1995) Controlling the false discovery rate: a practical and powerful approach to multiple testing. *J R Stat Soc B (Methodological)* 57:289–300.
- Blakemore SJ, Decety J (2001) From the perception of action to the understanding of intention. *Nat Rev Neurosci* 2:561–567.
- Bolsen T, Druckman JN, Fay, Cook L, Bolsen T, Druckman JN, Cook FL (2014) The influence of partisan motivated reasoning on public opinion. *Polit Behav* 36:235–262.
- Bruneau EG, Dufour N, Saxe R (2012) Social cognition in members of conflict groups: behavioural and neural responses in Arabs, Israelis and South Americans to each other's misfortunes. *Philos Trans R Soc Lond B Biol Sci* 367:717–730.
- Carney DR, Jost JT, Gosling SD, Potter J (2008) The secret lives of liberals and conservatives: personality profiles, interaction styles, and the things they leave behind. *Polit Psychol* 29:807–840.
- Cohen GL (2003) Party over policy: the dominating impact of group influence on political beliefs. *J Pers Soc Psychol* 85:808–822.
- Cortes C, Vapnik V (1995) Support-vector networks. *Mach Learn* 20:273–297.
- Dieffenthaler MC, Gillespie GS, Burns SM, McCulloh IA, Ames DL, Dagher MM, Falk EB, Lieberman MD, Wahbi Al Tal M (2021) Neural reference groups: a synchrony-based classification approach for predicting attitudes using fNIRS. *Soc Cogn Affect Neurosci* 16:117–128.
- Feldman J, Narayanan S (2004) Embodied meaning in a neural theory of language. *Brain Lang* 89:385–392.
- Finn ES, Corlett PR, Chen G, Bandettini PA, Constable RT (2018) Trait paranoia shapes inter-subject synchrony in brain activity during an ambiguous social narrative. *Nat Commun* 9:1–13.
- Finn ES, Glerean E, Khojandi AY, Nielson D, Molfese PJ, Handwerker DA, Bandettini PA (2020) Idiosynchrony: from shared responses to individual differences during naturalistic neuroimaging. *Neuroimage* 215:116828.
- Frederick SJ, Knowles ED, Saletan W, Loftus EF (2013) False memories of fabricated political events. *J Exp Soc Psychol* 49:280–286.
- Gallese V (2000) The inner sense of action. Agency and motor representations. *Journal of Consciousness studies* 7:23–40.
- Garbarini F, Adenzato M (2004) At the root of embodied cognition: cognitive science meets neurophysiology. *Brain Cogn* 56:100–106.
- Gorgolewski KJ, et al. (2016) The brain imaging data structure, a format for organizing and describing outputs of neuroimaging experiments. *Sci Data* 3:1–9.
- Hasson U, Nir Y, Levy I, Fuhrmann G, Malach R (2004) Intersubject synchronization of cortical activity during natural vision. *Science* 303:1634–1640.
- Hein G, Silani G, Preusschoff K, Batson CD, Singer T (2010) Neural responses to ingroup and outgroup members' suffering predict individual differences in costly helping. *Neuron* 68:149–160.
- Honey CJ, Thompson CR, Lerner Y, Hasson U (2012) Not lost in translation: neural responses shared across languages. *J Neurosci* 32:15277–15283.
- Jeannerod M (2001) Neural simulation of action: a unifying mechanism for motor cognition. *Neuroimage* 14:S103–S109.
- Jost JT, Amodio DM (2003) Political ideology as motivated social cognition: behavioral and neuroscientific evidence. *Person Soc Psychol Bull* 129:989–1007.
- Jost JT, Glaser J, Kruglanski AW, Sulloway FJ (2003) Political conservatism as motivated social cognition. *Psychol Bull* 129:339–375.
- Jost JT, van der Linden S, Panagopoulos C, Hardin CD (2018) Ideological asymmetries in conformity, desire for shared reality, and the spread of misinformation. *Curr Opin Psychol* 23:77–83.
- Kanai R, Feilden T, Firth C, Rees G (2011) Political orientations are correlated with brain structure in young adults. *Curr Biol* 21:677–680.
- Kraft PW, Lodge M, Taber CS (2015) Why people 'don't trust the evidence': motivated reasoning and scientific beliefs. *Ann Am Acad Polit Soc Sci* 658:121–133.
- Leonard NE, Lipsitz K, Bizyaeva A, Franci A, Lelkes Y (2021) The nonlinear feedback dynamics of asymmetric political polarization. *Proc Natl Acad Sci USA* 118:e2102149118.
- Leong YC, Chen J, Willer R, Zaki J (2020) Conservative and liberal attitudes drive polarized neural responses to political content. *Proc Natl Acad Sci USA* 117:27731–27739.
- Marino BF, Gallese V, Buccino G, Riggio L (2012) Language sensorimotor specificity modulates the motor system. *Cortex* 48:849–856.
- Mason L (2015) I disrespectfully agree: the differential effects of partisan sorting on social and issue polarization. *Am J Polit Sci* 59:128–145.
- Neumann R, Förster J, Strack F (2003) Motor compatibility: The bidirectional link between behavior and evaluation. *The psychology of evaluation: Affective processes in cognition and emotion.* (pp. 371–391). Lawrence Erlbaum Associates Publishers.
- Nguyen M, Vanderwal T, Hasson U (2019) Shared understanding of narratives is correlated with shared neural responses. *Neuroimage* 184:161–170.
- Pajula J, Tohka J (2016) How many is enough? Effect of sample size in inter-subject correlation analysis of fMRI. *Comput Intell Neurosci* 2016:2094601.
- Regev M, Honey CJ, Simony E, Hasson U (2013) Selective and invariant neural responses to spoken and written narratives. *J Neurosci* 33:15978–15988.
- Schmälzle R, Häcker FE, Honey CJ, Hasson U (2015) Engaged listeners: shared neural processing of powerful political speeches. *Soc Cogn Affect Neurosci* 10:1137–1143.
- Schreiber D, Fonzo G, Simmons AN, Dawes CT, Flagan T, Fowler JH, Paulus MP (2013) Red brain, blue brain: evaluative processes differ in Democrats and Republicans. *PLoS One* 8:e52970.
- Shen X, Tokoglu F, Papademetris X, Constable RT (2013) Groupwise whole-brain parcellation from resting-state fMRI data for network node identification. *Neuroimage* 82:403–415.
- Simony E, Honey CJ, Chen J, Lositsky O, Yeshurun Y, Wiesel A, Hasson U (2016) Dynamic reconfiguration of the default mode network during narrative comprehension. *Nat Commun* 7:1–13.
- Skerry AE, Saxe R (2015) Neural representations of emotion are organized around abstract event features. *Curr Biol* 25:1945–1954.
- Smith SM, Jenkinson M, Woolrich MW, Beckmann CF, Behrens TE, Johansen-Berg H, Bannister PR, de Luca M, Drobnjak I, Flitney DE, Niazy RK, Saunders J, Vickers J, Zhang Y, de Stefano N, Brady JM, Matthews PM (2004) Advances in functional and structural MR image analysis and implementation as FSL. *Neuroimage* 23:S208–S219.
- Tettamanti M, Buccino G, Saccuman MC, Gallese V, Danna M, Scifo P, Fazio F, Rizzolatti G, Cappa SF, Perani D (2005) Listening to action-related sentences activates fronto-parietal motor circuits. *J Cogn Neurosci* 17:273–281.
- van Baar JM, Halpern DJ, FeldmanHall O (2021) Intolerance of uncertainty modulates brain-to-brain synchrony during politically polarized perception. *Proc Natl Acad Sci USA* 118:e2022491118.
- van Bavel JJ, Pereira A (2018) The partisan brain: an identity-based model of political belief the role of identity in political belief. *Trends Cogn Sci* 22:213–224.
- van Overwalle F, Baetens K (2009) Understanding others' actions and goals by mirror and mentalizing systems: a meta-analysis. *Neuroimage* 48:564–584.
- Vigil JM (2010) Political leanings vary with facial expression processing and psychosocial functioning. *Group Process Intergroup Relations* 13:547–558.
- Xu X, Zuo X, Wang X, Han S (2009) Do you feel my pain? Racial group membership modulates empathic neural responses. *J Neurosci* 29:8525–8529.
- Yeshurun Y, Swanson S, Simony E, Chen J, Lazaridi C, Honey CJ, Hasson U (2017) Same story, different story: the neural representation of interpretive frameworks. *Psychol Sci* 28:307–319.